Z. Phys. C – Particles and Fields 51, 149–156 (1991)

Zeitschrift für Physik C Particles and Fields

A search for substructure of leptons and quarks with the CELLO detector

CELLO Collaboration

H.J. Behrend, L. Criegee, J.H. Field [1], G. Franke, H. Jung [2], J. Meyer, O. Podobrin, V. Schröder, G.G. Winter
Deutsches Elektronen-Synchrotron, DESY, Hamburg, Federal Republic of Germany

P.J. Bussey, C. Buttar [3], A.J. Campbell, D. Hendry, S. Lumsdon, I.O. Skillicorn

University of Glasgow, UK

J. Ahme, V. Blobel, M. Feindt, H. Fenner, J. Harjes, J. Köhne [4], J.H. Peters, H. Spitzer, T. Weihrich
II. Institut für Experimentalphysik, Universität, Hamburg, Federal Republic of Germany

W.D. Apel, J. Engler, G. Flügge [2], D.C. Fries, J. Fuster [5], K. Gamerdinger [6], P. Grosse-Wiesmann [7], H. Küster [8], H. Müller, K.H. Ranitzsch, H. Schneider
Kernforschungszentrum Karlsruhe und Universität, Karlsruhe, Federal Republic of Germany

W. de Boer [4], G. Buschhorn, G. Grindhammer, B. Gunderson, C. Kiesling, R. Kotthaus, H. Kroha [9], D. Lüers, H. Oberlack, P. Schacht, S. Scholz, W. Wiedenmann [7]
Max-Planck-Institut für Physik und Astrophysik, München, Federal Republic of Germany

M. Davier, J.F. Grivaz, J. Haissinski, V. Journé, F. Le Diberder [10], J.J. Veillet
Laboratoire de l'Accélérateur Linéaire, Orsay, France

K. Blohm, R. George, M. Goldberg, O. Hamon, F. Kapusta, L. Poggioli, M. Rivoal
Laboratoire de Physique Nucléaire et Hautes Energies, Université de Paris, Paris, France

G. d'Agostini, F. Ferrarotto, M. Iacovacci, G. Shooshtari, B. Stella
Università di Roma and INFN, Rome, Italy

G. Cozzika, Y. Ducros
Centre d'Etudes Nucléaires, Saclay, France

G. Alexander, A. Beck, G. Bella, J. Grunhaus, A. Klatchko [11], A. Levy, C. Milstène
Tel Aviv University, Tel Aviv, Israel

Received 16 November 1990

Present addresses:
[1] Université de Genève, Switzerland
[2] RWTH, Aachen, FRG
[3] Sheffield Univ., UK
[4] Univ. Karlsruhe, FRG
[5] Instituto de Física Corpuscular, Universidad de Valencia, Spain
[6] MPI für Physik und Astrophysik, München, FRG
[7] CERN, Geneva, Switzerland
[8] DESY, Hamburg, FRG
[9] Univ. of Rochester, USA
[10] Stanford Linear Accelerator Center, Stanford, USA
[11] Univ. of California at Riverside, USA

Abstract. Differential cross section data of the CELLO experiment on pair production of muons, taus, and heavy quarks in e^+e^--annihilation are presented and analysed, together with our data on Bhabha scattering, in terms of compositeness effects characterized by the mass scale Λ. We discuss difficulties in the combination of limits Λ from different experiments. The appropriate parameter to combine different results turns out to be $\varepsilon = \pm 1/\Lambda^2$, which is in contrast to Λ Gaussian distributed.

1 Introduction

Any substructure of leptons and quarks induces a new effective 4-fermion contact interaction [1]. Under very general conditions (chirality and flavour conservation, exact validity of the standard model gauge structure, i.e. no composite gauge bosons) e^+e^- annihilation into fermion pairs $f\bar{f}$ via contact interaction is described by the Lagrangian

$$\mathcal{L}^{ef}_{\text{contact}} = \frac{g^2}{\Lambda^2} \sum_{i,j=\text{L,R}} \eta_{ij} [\bar{e}_i \gamma^\mu e_i][\bar{f}_j \gamma_\mu f_j] \tag{1}$$

with the compositeness scale Λ and the convention $g^2/4\pi = 1$ for the unknown coupling constant. The parameters $\eta_{ij} = 0, \pm 1$ define the type of $eeff$ chiral coupling.

The interference of the contact term with the standard model Born processes results in the differential cross section

$$\frac{4s}{\alpha^2}\frac{\mathrm{d}\sigma^{ff}}{\mathrm{d}\Omega} = 2|\tilde{\mathcal{A}}^{ee}_{\text{LR}}|^2 \left(\frac{s}{t}\right)^2 \cdot \delta_{ef} + [|\mathcal{A}^{ef}_{\text{LR}}|^2 + |\mathcal{A}^{ef}_{\text{RL}}|^2]\left(\frac{t}{s}\right)^2 + [|\mathcal{A}^{ef}_{\text{LL}}|^2 + |\mathcal{A}^{ef}_{\text{RR}}|^2]\left(\frac{u}{s}\right)^2 \tag{2}$$

with $\delta_{ef} = 1$ (0) for $f = e (f \neq e)$, $t = -s/2 \cdot (1 - \cos\theta)$, and $s + t + u = 0$, and with the helicity amplitudes

$$\begin{aligned}
\tilde{\mathcal{A}}^{ee}_{\text{LR}} &= Q_e^2 + c^e_{\text{L}} c^e_{\text{R}} \chi(t) + \frac{\eta_{\text{RL}}}{\alpha}\frac{t}{\Lambda^2} \equiv \tilde{\mathcal{A}}^{ee}_{\text{RL}};\\
\mathcal{A}^{ef}_{ij} &= Q_e Q_f + c^e_i c^f_j \chi(s) + \frac{\eta_{ij}}{\alpha}\frac{s}{\Lambda^2}; \quad (i \neq j)\\
\mathcal{A}^{ef}_{ij} &= Q_e Q_f + c^e_i c^f_j \left[\chi(s) + \frac{s}{t}\chi(t)\cdot\delta_{ef}\right]\\
&\quad + \frac{s}{t}\cdot\delta_{ef} + (1+\delta_{ef})\cdot\frac{\eta_{ij}}{\alpha}\frac{s}{\Lambda^2}; \quad (i = j).
\end{aligned} \tag{3}$$

$c^f_{\text{L,R}}$ are the left and right handed couplings of the fermions to the Z^0 boson and $\chi(y) \sim y/(y - M_Z^2 + iM_Z\Gamma_Z)$ is the Z^0 propagator. The following models have been considered:

$\Lambda^\pm_{\text{LL}}$: $\eta_{\text{LL}} = \pm 1, \eta_{\text{RR}} = \eta_{\text{LR}} = \eta_{\text{RL}} = 0$;
$\Lambda^\pm_{\text{RR}}$: $\eta_{\text{RR}} = \pm 1, \eta_{\text{LL}} = \eta_{\text{LR}} = \eta_{\text{RL}} = 0$;
$\Lambda^\pm_{\text{AA}}$: $\eta_{\text{LL}} = \eta_{\text{RR}} = -\eta_{\text{LR}} = -\eta_{\text{RL}} = \pm 1$;
$\Lambda^\pm_{\text{VV}}$: $\eta_{\text{LL}} = \eta_{\text{RR}} = \eta_{\text{LR}} = \eta_{\text{RL}} = \pm 1$;
$\Lambda^\pm_{\text{LR}}$: $\eta_{\text{LR}} = \pm 1, \eta_{\text{LL}} = \eta_{\text{RR}} = \eta_{\text{RL}} = 0$;
$\Lambda^\pm_{\text{RL}}$: $\eta_{\text{RL}} = \pm 1, \eta_{\text{LL}} = \eta_{\text{RR}} = \eta_{\text{LR}} = 0$.

It should be noted that $\Lambda^\pm_{\text{LL}} \approx \Lambda^\pm_{\text{RR}}$ for present experimental resolution (see below) and that $\Lambda^\pm_{\text{LR}} \equiv \Lambda^\pm_{\text{RL}}$ for all leptonic but *not* for quark final states.

The terms in equations (2, 3) proportional to $\varepsilon = \pm\Lambda^{-2}$ constitute the deviations from the standard model (GSW) prediction. They are determined by fitting to the measured differential cross sections for fermion pair production the expectation (2) with $M_Z = 91.17$ GeV, $\sin^2\theta_W = 0.2307$ and with ε as free parameter. Measurement and expectation are normalized to the standard model prediction (obtained from (2, 3) for $\Lambda \mapsto \infty$). From the fits of ε lower limits on $\Lambda^\pm$ can be derived.

2 Data sample

We have investigated the CELLO data on Bhabha scattering at $\sqrt{s} = 35$ GeV, on muon, tau and heavy quark production at $\sqrt{s} = 35$ and 43 GeV, with an integrated luminosity of 87 pb^{-1} at 35 GeV and 48.7 pb^{-1} at 43 GeV. Bhabha scattering provides a test for the compositeness of electrons alone, which has recently been published by CELLO [2]. For other final state fermions in e^+e^- annihilation the additional (but reasonable) assumption of a common substructure with the electron has to be made.

The muon and tau pair production cross sections are listed in Tables 1 and 2. The errors include systematic effects due to background substraction (2%), radiative corrections (0.2%), and overall efficiency uncertainties (2%). The additional normalisation errors are dominated by the uncertainty of the luminosity determination (3%). Details of the measurements can be found elsewhere [3, 4].

The heavy quark cross sections allow a separate investigation of the common substructure of the charm and the bottom quark with the electron, which might

Table 1. Corrected differential cross sections for muon pair production at $\sqrt{s} = 35$ and 43 GeV. Statistical and systematic errors have been added quadratically

$\sqrt{s} = 35$ GeV		$\sqrt{s} = 43$ GeV	
$\langle\cos\theta\rangle$	$s(\mathrm{d}\sigma/\mathrm{d}\Omega)\cdot(e^+e^-\to\mu^+\mu^-)$ [nb·GeV^2/sterad]	$\cos\theta$	$s(\mathrm{d}\sigma/\mathrm{d}\Omega)\cdot(e^+e^-\to\mu^+\mu^-)$ [nb·GeV^2/sterad]
−0.765	7.84±0.44	−0.744	9.24±0.81
−0.595	8.39±0.47	−0.531	7.41±0.72
−0.425	6.32±0.40	−0.319	5.06±0.62
−0.255	5.83±0.39		
−0.085	5.32±0.38	−0.106	5.42±0.67
+0.085	5.12±0.36	+0.106	4.50±0.63
+0.255	4.56±0.33		
+0.425	4.97±0.35	+0.319	4.62±0.56
+0.595	6.13±0.37	+0.531	5.00±0.57
+0.765	7.17±0.39	+0.744	6.44±0.61

Table 2. Corrected differential cross sections for tau pair production at $\sqrt{s} = 35$ and 43 GeV. Statistical and systematic errors have been added quadratically

$\langle\cos\theta\rangle$	$s(\mathrm{d}\sigma/\mathrm{d}\Omega)(e^+e^-\to\tau^+\tau^-)$ [nb·GeV^2/sterad]	
	$\sqrt{s} = 35$ GeV	$\sqrt{s} = 45$ GeV
−0.70	8.24±0.39	10.24±0.79
−0.50	6.97±0.36	7.16±0.64
−0.30	6.11±0.33	6.08±0.58
−0.10	5.54±0.32	4.87±0.52
+0.10	5.10±0.29	3.87±0.47
+0.30	5.95±0.33	5.55±0.56
+0.50	5.93±0.33	5.88±0.52
+0.70	7.00±0.36	6.25±0.59

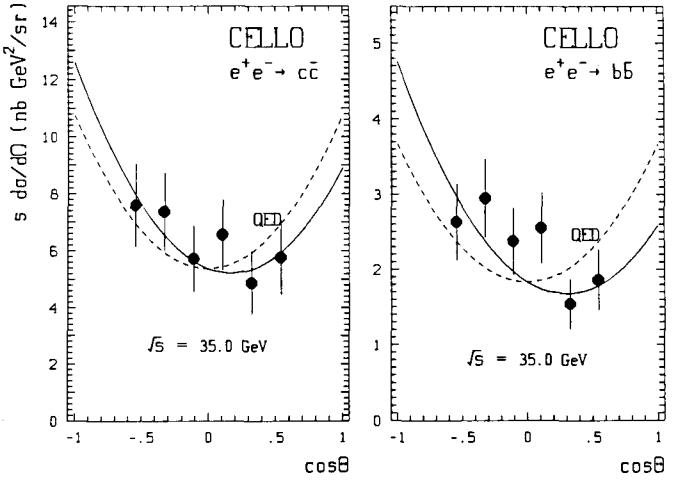

Fig. 1. Corrected differential cross section for charm and bottom quark pair production at $\sqrt{s}=35$ GeV. The error bars include statistical and systematic uncertainties. No corrections for $B^0\overline{B^0}$ mixing have been applied

Table 3. Corrected differential cross sections for charm and bottom quark pair production at $\sqrt{s}=35$ GeV. B^0B^0 mixing corrections are not included. Statistical and systematic errors have been added quadratically

$\langle\cos\theta\rangle$	$s(d\sigma/d\Omega)(e^+e^-\to c\bar{c})$ [nb·GeV^2/sterad]	$s(d\sigma/d\Omega)(e^+e^-\to b\bar{b})$ [nb·GeV^2/sterad]
−0.542	7.60±1.15	2.63±0.41
−0.325	7.37±1.04	2.95±0.41
−0.108	5.73±0.93	2.38±0.36
+0.108	6.56±0.97	2.55±0.37
+0.325	4.88±0.95	1.54±0.28
+0.542	5.78±1.12	1.86±0.38

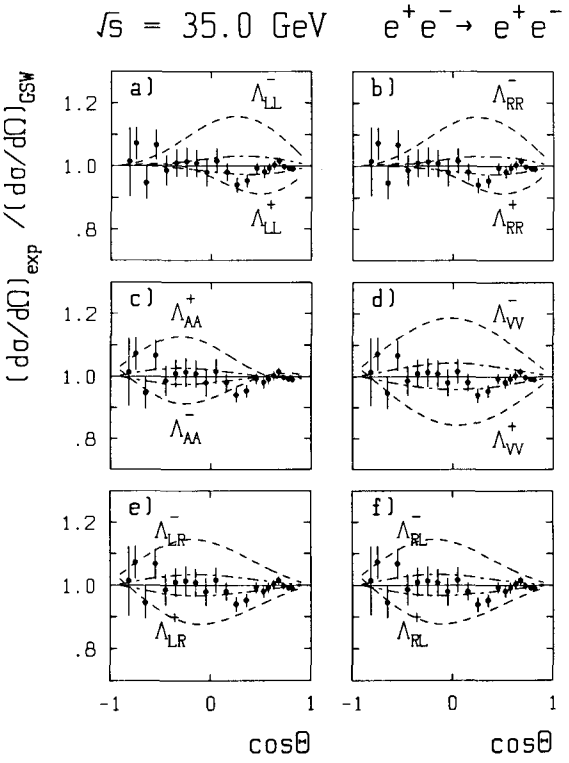

Fig. 2. Bhabha cross section at $\sqrt{s}=35$ GeV normalized to the standard model prediction in comparison with the expectations from additional contact interactions with different types of chiral couplings (the dashed curves are for $\Lambda=0.5$ TeV in a) and b) and for $\Lambda=1.0$ TeV in c), d), e), f); the dashed-dotted curves are for $\Lambda=1.0$ TeV in a) and b) and for $\Lambda=2.0$ TeV in c), d), e), f), respectively). The common relative normalization error of 2.5% is not included in the error bars

appear at a scale different from that for lighter quarks [5]. For cross section measurements the $c\bar{c}$ and $b\bar{b}$ pair production has been identified by fitting to the multidimensional distributions of several separating variables: the transverse momentum p_T of prompt electrons and muons with respect to the thrust axis, the sum $\sum p_T^{out}$ of all particles perpendicular to the event plane, and the energy fraction E_{corr} inside a certain cone around the identified lepton (see [6, 7] for details). Systematic errors of the quark flavour identification have been determined for each individual $\cos\theta$ bin using the same methods and variations of parameters as described in [6]. On the average the relative systematic errors amount to 10–15%. The differential cross sections for c and b production at $\sqrt{s}=35$ GeV are shown in Fig. 1. Additional relative normalization errors common to all bins amount to 5% for the efficiencies, 2.5% for the luminosity determined from forward Bhabha scattering, and 10% for the world average semileptonic branching ratios of the c and b-quark. From a fit of the Born level prediction of the standard model

$$\frac{d\sigma^{q\bar{q}}}{d\Omega}=R_q[\tfrac{3}{8}(1+\cos^2\theta)+A_{FB}^q\cos\theta] \quad (4)$$

to the corrected data shown in Table 3 and Fig. 1 we obtain values (and errors) for the charm and bottom charge asymmetries $A_{FB}^{c,b}$ in very good agreement with the previous results from the direct fit [6] and values for the total cross sections $R_{c,b}$ relative to the lowest order muon pair cross section which are consistent with the standard model prediction (Table 4). The $b\bar{b}$ cross

Table 4. The charge asymmetries, the semileptonic branching ratios, and the total cross section at $\sqrt{s}=35$ GeV for charm and bottom quark pair production from the direct fit and via the determination of the differential cross section as function of $\cos\theta$. In both cases, the b asymmetry is not corrected for $B^0\overline{B^0}$ mixing. Statistical and systematic errors are combined

$q\to l$ ($l=e,\mu$)	BR [%] direct fit	A_{FB}^q [%] direct fit	A_{FB}^q [%] from $d\sigma/d\Omega$	A_{FB}^q [%] GSW Born	R_q from $d\sigma/d\Omega$	R_q GSW Born
$b\to l$	14.9±1.5	−(22.2±8.1)	−(22.2±8.3)	−26.0	0.35±0.05	0.34
$c\to l$	7.1±0.7	−(12.9±8.8)	−(14.6±8.4)	−13.6	1.04±0.14	1.34

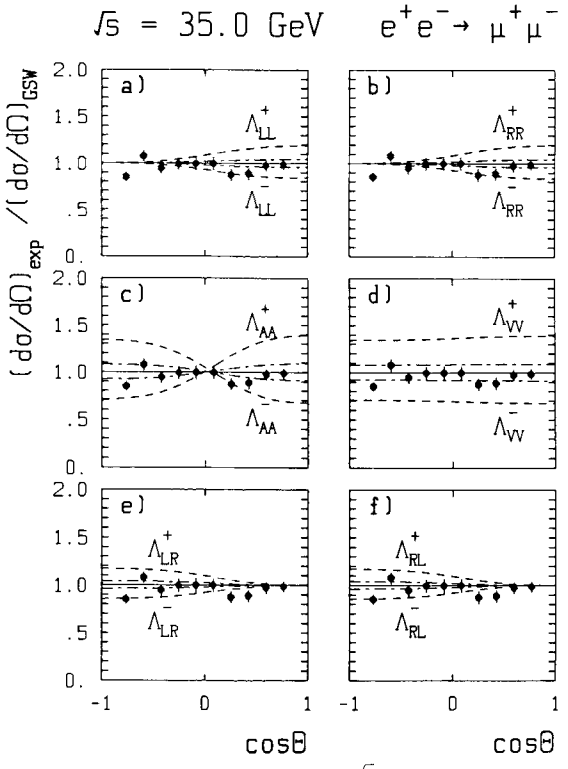

Fig. 3. Muon pair cross section at $\sqrt{s}=35$ GeV normalized to the standard model prediction in comparison with the expectations from additional contact interactions with different types of chiral couplings (the dashed curves are for $\Lambda=1.0$ TeV and the dashed-dotted curves for $\Lambda=2.0$ TeV). The common relative normalization error of 5.0% is not included in the error bars

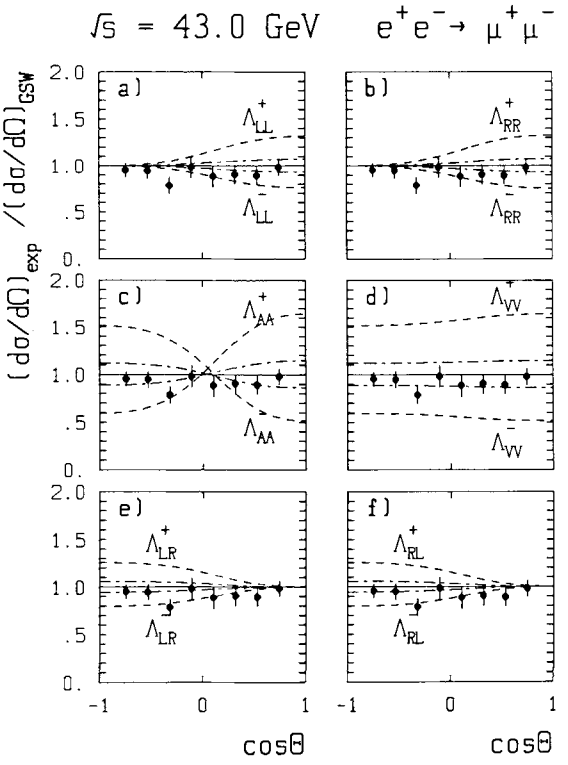

Fig. 4. Muon pair cross section at $\sqrt{s}=43$ GeV normalized to the standard model prediction in comparison with the expectations from additional contact interactions with different types of chiral couplings (the dashed curves are for $\Lambda=1.0$ TeV and the dashed-dotted curves for $\Lambda=2.0$ TeV). The common relative normalization error of 4.1% is not included in the error bars

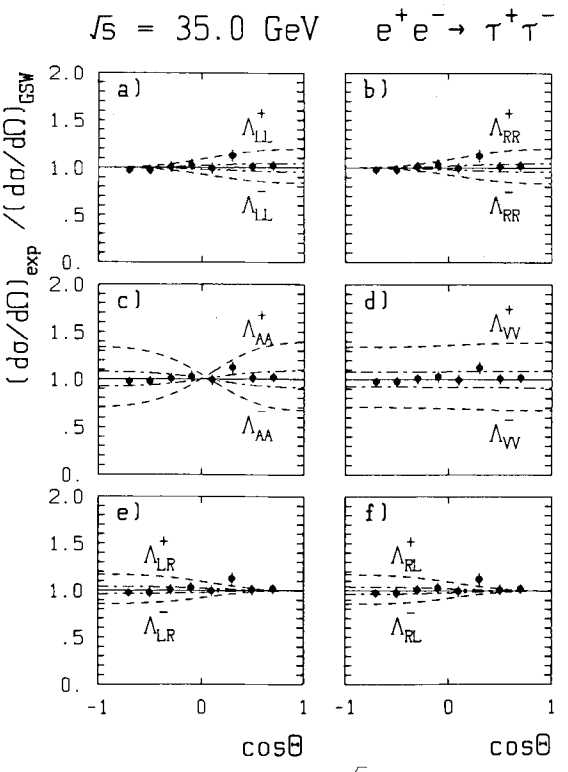

Fig. 5. Tau pair cross section at $\sqrt{s}=35$ GeV normalized to the standard model prediction in comparison with the expectations from additional contact interactions with different types of chiral couplings (the dashed curves are for $\Lambda=1.0$ TeV and the dashed-dotted curves for $\Lambda=2.0$ TeV). The common relative normalization error of 2.8% is not included in the error bars

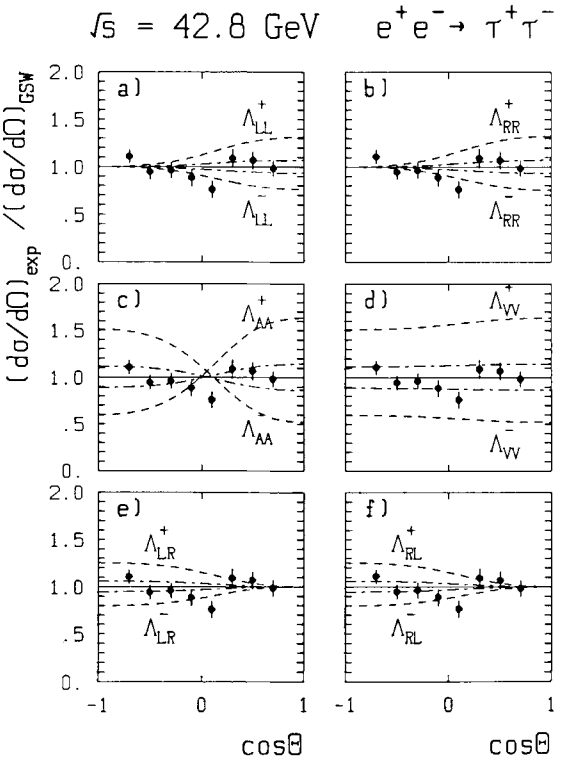

Fig. 6. Tau pair cross section at $\sqrt{s}=42.8$ GeV normalized to the standard model prediction in comparison with the expectations from additional contact interactions with different types of chiral couplings (the dashed curves are for $\Lambda=1.0$ TeV and the dashed-dotted curves for $\Lambda=2.0$ TeV). The common relative normalization error of 4.0% is not included in the error bars

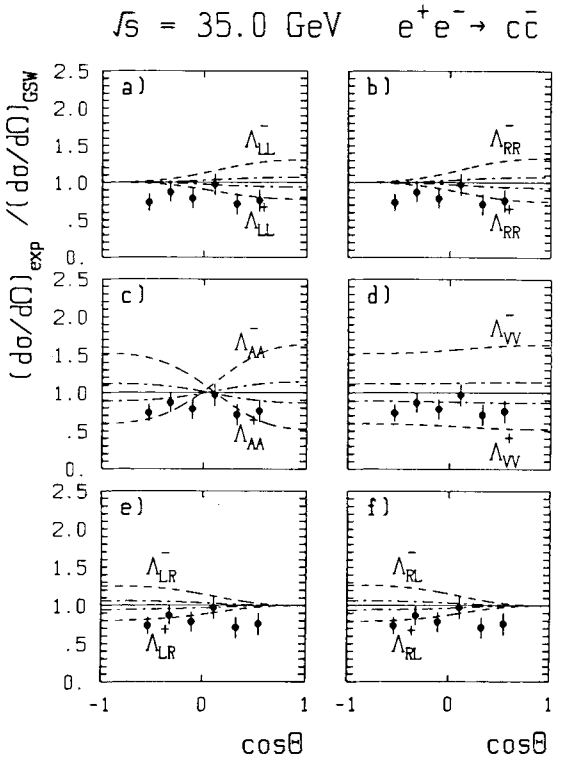

Fig. 7. $c\bar{c}$ cross section at $\sqrt{s}=42.8$ GeV normalized to the standard model prediction in comparison with the expectations from additional contact interactions with different types of chiral couplings (the dashed curves are for $\Lambda=1.0$ TeV and the dashed-dotted curves for $\Lambda=2.0$ TeV). The common relative normalization error of 11.6% is not included in the error bars

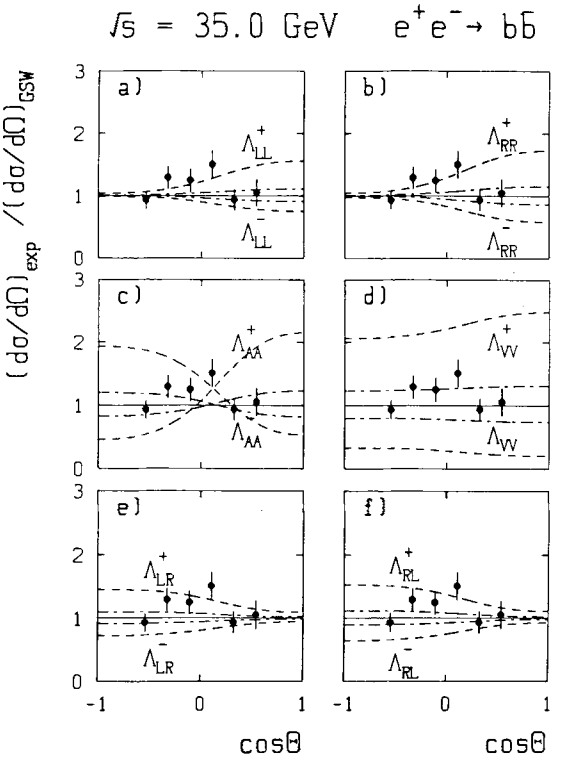

Fig. 8. $b\bar{b}$ cross section at $\sqrt{s}=42.8$ GeV normalized to the standard model prediction in comparison with the expectations from additional contact interactions with different types of chiral couplings (the dashed curves are for $\Lambda=1.0$ TeV and the dashed-dotted curves for $\Lambda=2.0$ TeV). The common relative normalization error of 11.1% is not included in the error bars. $B^0\overline{B^0}$ mixing is taken into account in the measured and the expected cross section ratios. The uncertainty in the correction is included in the errors

section includes correction due to $B^0\overline{B^0}$ mixing using for the mixing parameter $\chi_l=0.10\pm0.04$ from the combined measurements of UA1 [8], ARGUS [9] and CLEO [10]. The statistically poor results for the heavy quark production cross sections at $\sqrt{s}=43$ GeV have not been included in the compositeness studies. The sensitivity of the data to the various compositeness scales introduced in the previous section is displayed in Figs. 2–8.

3 Fitting methods

The fit to the differential cross section ratio $y=\dfrac{\mathrm{d}\sigma}{\mathrm{d}\Omega_{\mathrm{obs}}}\Big/\dfrac{\mathrm{d}\sigma}{\mathrm{d}\Omega_{\mathrm{GSW}}}$ is sensitive to both its shape and normalization. Two alternative methods can be used to take into account common normalization errors of the data points due to uncertainties in the luminosity and in trigger and detection efficiencies:

(A) The method applied in all previous measurements introduces an additional free normalization parameter n in the definition of the χ^2 function:

$$\chi^2=\sum_{i=1}^{N}\frac{(n\,y_i-y_i^{\mathrm{th}})^2}{(n\sigma_i)^2}+\frac{(1-n)^2}{\sigma_n^2}. \tag{5}$$

(B) The correlations introduced by the common normalization uncertainty can also be taken into account by using in

$$\chi^2=\sum_{i,j=1}^{N}(y_i-y_i^{\mathrm{th}})\,C_{ij}^{-1}(y_j-y_j^{\mathrm{th}}) \tag{6}$$

the full covariance matrix estimated by

$$C_{ii}=\sigma_i^2+\sigma_n^2\cdot y_i^2$$
$$C_{ij}=\sigma_n^2\cdot y_i y_j \quad (i\neq j) \tag{7}$$

(compare [11] for a recent application of this method in a combined fit of total hadronic cross section measurements).

The independent point-to-point errors $\sigma_i^2=\sigma_{\mathrm{stat}\,i}^2+\sigma_{\mathrm{syst}\,i}^2$ do not contain the relative normalization uncertainty σ_n. Both methods are completely equivalent (compare [12]) if the data points y_i in (7) are replaced by their expectation values $\langle y_i\rangle$ which a priori are not known.

Method (A) is a straight forward implementation of the correlations induced by common normalization uncertainties. But one has to introduce at least one additional normalization parameter for each $\mathrm{d}\sigma/\mathrm{d}\Omega$ measurement in a combined analysis. In contrast, the covariance matrix method (B) allows to take into account even correlations between different cross section measurements without the need of additional fitting parameters. How-

ever, it turns out, as shown below, that these correlations have only a minor influence on the resulting compositeness limits.

4 Results and discussion

From fits to the measured cross sections, we obtain for the various choices of chiral couplings the values of $\varepsilon = \pm \Lambda^{-2}$ given in Tables 5 and 6. In these fits for ε, a global positive sign for the η parameters in (3) was imposed. Results are shown for possible $eeee$, $ee\mu\mu$, $ee\tau\tau$, $eecc$, and $eebb$ contact interactions separately, as well as for all final state lepton types combined. Including also the measurements for heavy quarks does not change the results significantly. The sensitivity of the bottom quark cross section to effects of new contact interactions is, however, not far below that of the higher statistics lepton data since the predicted effects for quark pair production are considerably larger.

The results using the free normalization (fn) or the full covariance matrix (cov) method are in general in good agreement with one another. The fitted normalization parameters n_k ($k = 1, \ldots, N_{\text{exp}}$) are all consistent with

Table 5. Results of the fit for the parameter $\varepsilon = \pm 1/\Lambda^2$ [TeV^{-2}] with the covariance matrix method (cov) and with free normalization (fn) for lepton data

	e^+e^-	$\mu^+\mu^-$	$\tau^+\tau^-$	l^+l^-
LL cov	$+(0.904 \pm 0.593)$	$-(0.184 \pm 0.190)$	$+(0.069 \pm 0.178)$	$+(0.036 \pm 0.113)$
LL fn	$+(0.791 \pm 0.583)$	$-(0.144 \pm 0.192)$	$+(0.108 \pm 0.178)$	$+(0.030 \pm 0.126)$
RR cov	$+(0.901 \pm 0.597)$	$-(0.179 \pm 0.185)$	$+(0.066 \pm 0.174)$	$+(0.033 \pm 0.111)$
RR fn	$+(0.787 \pm 0.589)$	$-(0.140 \pm 0.186)$	$+(0.104 \pm 0.173)$	$+(0.026 \pm 0.123)$
AA cov	$-(0.070 \pm 0.147)$	$+(0.016 \pm 0.056)$	$+(0.049 \pm 0.058)$	$+(0.023 \pm 0.039)$
AA fn	$-(0.069 \pm 0.148)$	$+(0.016 \pm 0.058)$	$+(0.049 \pm 0.058)$	$+(0.025 \pm 0.039)$
VV cov	$+(0.152 \pm 0.103)$	$-(0.189 \pm 0.087)$	$-(0.030 \pm 0.071)$	$-(0.007 \pm 0.039)$
VV fn	$+(0.137 \pm 0.101)$	$-(0.153 \pm 0.086)$	$-(0.004 \pm 0.071)$	$-(0.020 \pm 0.048)$
LR cov	$+(0.152 \pm 0.132)$	$-(0.308 \pm 0.204)$	$-(0.169 \pm 0.187)$	$+(0.001 \pm 0.082)$
LR fn	$+(0.139 \pm 0.131)$	$-(0.258 \pm 0.204)$	$-(0.127 \pm 0.185)$	$-(0.016 \pm 0.092)$

Table 6. Results of the fit for the parameter $\varepsilon = \pm 1/\Lambda^2$ [TeV^{-2}] with the covariance matrix method (cov) and with free normalization (fn) for heavy quark and combined lepton and heavy quark data

	$c\bar{c}$	$b\bar{b}$	$(c\bar{c}, b\bar{b})$	$l^+l^- + q\bar{q}$
LL cov	$+\left(0.841^{+1.120}_{-0.623}\right)$	$-\left(0.001^{+0.453}_{-0.718}\right)$	$+\left(0.285^{+0.315}_{-0.342}\right)$	$+(0.060 \pm 0.107)$
LL fn	$+\left(0.766^{+0.875}_{-0.696}\right)$	$+\left(0.176^{+0.427}_{-0.540}\right)$	$+\left(0.344^{+0.343}_{-0.367}\right)$	$+(0.062 \pm 0.119)$
RR cov	$+\left(0.746^{+0.802}_{-0.554}\right)$	$-\left(0.0004^{+0.341}_{-0.417}\right)$	$+\left(0.206^{+0.261}_{-0.279}\right)$	$+(0.056 \pm 0.102)$
RR fn	$+\left(0.682^{+0.716}_{-0.617}\right)$	$+\left(0.128^{+0.336}_{-0.364}\right)$	$+\left(0.258^{+0.286}_{-0.295}\right)$	$+(0.060 \pm 0.113)$
AA cov	$-\left(0.015^{+0.168}_{-0.167}\right)$	$-\left(0.032^{+0.160}_{-0.162}\right)$	$-\left(0.024^{+0.116}_{-0.116}\right)$	$+(0.018 \pm 0.037)$
AA fn	$-\left(0.015^{+0.199}_{-0.195}\right)$	$-\left(0.054^{+0.151}_{-0.162}\right)$	$-\left(0.039^{+0.120}_{-0.123}\right)$	$+(0.018 \pm 0.038)$
VV cov	$+\left(0.481^{+0.252}_{-0.225}\right)$	$+\left(0.024^{+0.136}_{-0.146}\right)$	$+\left(0.148^{+0.108}_{-0.111}\right)$	$+(0.010 \pm 0.037)$
VV fn	$+\left(0.422^{+0.240}_{-0.236}\right)$	$+\left(0.114^{+0.138}_{-0.141}\right)$	$+\left(0.193^{+0.118}_{-0.119}\right)$	$+(0.010 \pm 0.045)$
LR cov	$+\left(0.907^{+0.912}_{-0.612}\right)$	$+\left(0.113^{+0.401}_{-0.491}\right)$	$+\left(0.351^{+0.304}_{-0.323}\right)$	$+(0.020 \pm 0.080)$
LR fn	$+\left(0.772^{+0.733}_{-0.647}\right)$	$+\left(0.346^{+0.392}_{-0.431}\right)$	$+\left(0.462^{+0.329}_{-0.341}\right)$	$+(0.015 \pm 0.090)$
RL cov	$+\left(0.851^{+0.785}_{-0.574}\right)$	$+\left(0.094^{+0.344}_{-0.396}\right)$	$+\left(0.296^{+0.272}_{-0.286}\right)$	$+(0.022 \pm 0.079)$
RL fn	$+\left(0.726^{+0.667}_{-0.606}\right)$	$+\left(0.926^{+0.344}_{-0.362}\right)$	$+\left(0.399^{+0.295}_{-0.301}\right)$	$+(0.019 \pm 0.089)$

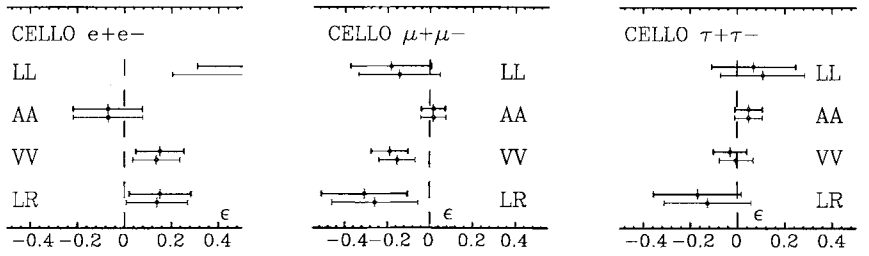

Fig. 9. Results of the fit for the parameter $\varepsilon = \pm 1/\Lambda^2$ [TeV^{-2}] with the covariance matrix method (thick bars) and with free normalization (thin bars) for lepton data

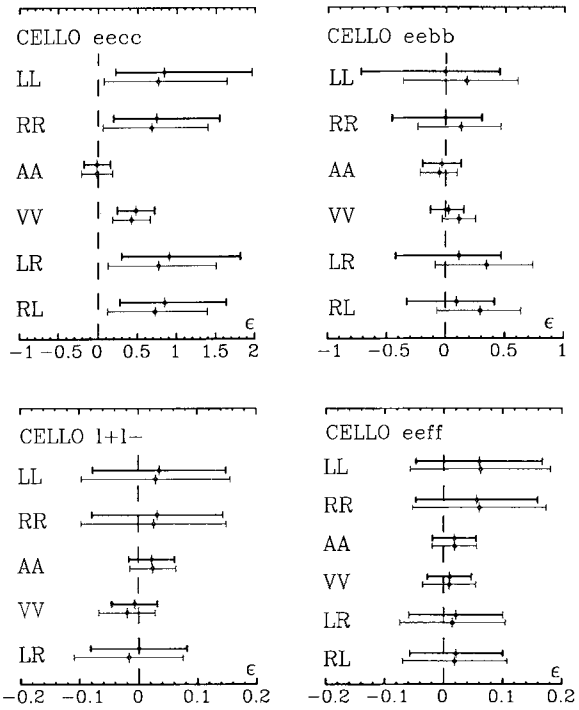

Fig. 10. Results of the fit for the parameter $\varepsilon = \pm 1/\Lambda^2$ [TeV^{-2}] with the covariance matrix method (thick bars) and with free normalization (thin bars) for heavy quark and combined lepton and fermion data

unity well within their errors despite the larger number N_{exp} of combined measurements ($N_{exp}=7$ for the combined lepton and quark data). Correlations between different $d\sigma/d\Omega$ distributions have been taken into account for the measurements at $\sqrt{s}=35$ and 43 GeV, respectively, due to the common uncertainty in the luminosity at each energy (2.5% and 3.0%, respectively). The comparison of the combined lepton results with both methods (see Tables 5 and 6, Figs. 9 and 10) shows that the correlations between different differential cross sections have only a minor influence on the results.

Figures 9 and 10 illustrate the degree of agreement between the measurements and the standard model. Though fluctuations around the GSW prediction can be seen, the fit results are compatible with $\varepsilon=0$. Note that the size and cos θ dependent shape of the deviations from the standard model predicted for additional contact interactions vary considerably for different types of chiral couplings (compare Figs. 2–8). The level of agreement cannot be judged from limits on the compositeness scale Λ alone which have exclusively been given in all previous

Table 7a. Lower limits on the compositeness scale Λ [TeV] at 95% C.L. from leptonic final states

	e^+e^-		$\mu^+\mu^-$		$\tau^+\tau^-$		l^+l^-	
	cov	fn	cov	fn	cov	fn	cov	fn
Λ^+_{LL}	0.7	0.7	2.9	2.5	1.7	1.6	2.1	2.1
Λ^-_{LL}	6.8	2.8	1.4	1.5	2.1	2.3	2.6	2.4
Λ^+_{RR}	0.7	0.7	3.0	2.5	1.7	1.6	2.2	2.1
Λ^-_{RR}	5.5	2.6	1.4	1.5	2.1	2.3	2.6	2.4
Λ^+_{AA}	2.5	2.5	3.1	3.0	2.6	2.6	3.4	3.3
Λ^-_{AA}	1.8	1.8	3.6	3.5	4.6	4.6	5.0	5.0
Λ^+_{VV}	1.8	1.8	–	–	3.4	3.0	4.2	4.1
Λ^-_{VV}	8.7	5.8	1.7	1.8	2.6	2.9	3.8	3.2
Λ^+_{LR}	1.6	1.7	8.1	3.8	2.8	2.4	2.7	2.7
Λ^-_{LR}	4.1	3.7	1.2	1.3	1.4	1.5	2.7	2.4

Table 7b. Lower limits on the compositeness scale Λ [TeV] at 95% C.L. from quark final states and for all fermions combined

	$c\bar{c}$		$b\bar{b}$		$c\bar{c}+b\bar{b}$		$l^+l^-+q\bar{q}$	
	cov	fn	cov	fn	cov	fn	cov	fn
Λ^+_{LL}	0.6	0.6	1.2	1.1	1.1	1.1	2.1	2.0
Λ^-_{LL}	2.4	1.7	0.9	1.0	1.8	1.9	2.9	2.7
Λ^+_{RR}	0.7	0.7	1.4	1.2	1.3	1.2	2.1	2.0
Λ^-_{RR}	2.5	1.8	1.2	1.4	2.0	2.1	3.0	2.8
Λ^+_{AA}	2.0	1.8	2.1	2.3	2.5	2.5	3.6	3.5
Λ^-_{AA}	1.9	1.7	1.8	1.7	2.2	2.0	4.9	4.8
Λ^+_{VV}	1.1	1.1	2.0	1.7	1.8	1.6	3.8	3.5
Λ^-_{VV}	–	–	2.1	2.9	5.3	19.0	4.4	4.0
Λ^+_{LR}	0.6	0.7	1.2	1.0	1.1	1.0	2.6	2.5
Λ^-_{LR}	3.2	2.0	1.1	1.6	2.3	3.1	3.0	2.8
Λ^+_{RL}	0.7	0.7	1.3	1.1	1.2	1.1	2.6	2.5
Λ^-_{RL}	3.3	2.0	1.3	1.8	2.4	3.2	3.0	2.8

measurements. Lower limits on Λ at 95% C.L. can be derived from the fitted ε values according to the relation

$$\Lambda^{\pm}_{limit} = 1/\sqrt{1.64\sigma_\varepsilon \pm \varepsilon} \qquad (8)$$

(the $1.64\sigma_\varepsilon$ errors correspond to $\chi^2_{min} \mapsto \chi^2_{min} + 2.69$). The results are summarized in Table 7.

It is important to note that while ε is Gaussian distributed to a good approximation the errors on the scale Λ itself are non-Gaussian. Even small fluctuations in the data, resulting in deviations of the contact terms ($\sim\varepsilon$) from zero that are still compatible with the standard model can have dramatic effects on Λ. It is not unusual

that they lead to very asymmetric results for the limits on Λ^+ and Λ^- where the limit with sign opposite to that of ε can then be very large compared to the experimental resolution or even does not exist at the given confidence level (negative sign under the square root in (8) and the dashes in Table 7).

5 Conclusions

We have measured the differential cross sections for muon, tau, charm and bottom pair production at center of mass energies of 35 and 43 GeV, using the CELLO detector at PETRA. Together with our data from Bhabha scattering these cross sections have been analysed for possible fermion substructure. No significant deviations of fermion pair production from the standard model prediction have been observed. The compositeness scale Λ usually given by experiments does not seem to be the appropriate parameter to estimate effects of possible new contact interactions: Λ limits from different experiments cannot easily be compared or combined. Extremely high limits on Λ are usually due to statistical fluctuations in the data and should be taken with caution. For more reliable comparison, the results for the fitted parameter $\varepsilon = \pm 1/\Lambda^2$ with errors, i.e. the experimental resolution power, have been given for each cross section. Such numbers, we suggest, should also be provided by other experiments.

Acknowledgements. We gratefully acknowledge the outstanding efforts of the PETRA machine group which made possible these measurements. We are indebted to the DESY computer centre for their excellent support during the experiment. We acknowledge the invaluable effort of the many engineers and technicians from the collaborating institutions in the construction and maintenance of the apparatus. The visiting groups wish to thank the DESY Directorate for the support and kind hospitality extended to them. This work was partially supported by the Bundesministerium für Forschung und Technologie (Federal Republic of Germany), by the Commissariat à l'Energie Atomique and the Institut National de Physique Nucléaire et de Physique des Particules (France), by the Istituto Nazionale di Fisica Nucleare (Italy), by the Science and Engineering Research Council (UK), and by the Ministry of Science and Development (Israel).

References

1. E.J. Eichten, K.D. Lane, M.E. Peskin: Phys. Rev. Lett. 50 (1983) 811; E. Eichten, I. Hinchliffe, K. Lane, C. Quigg: Rev. Mod. Phys. 56 (1984) 579
2. CELLO Coll. H.J. Behrend et al.: Z. Phys. C – Particles and Fields 51 (1990) 142
3. CELLO Coll. H.J. Behrend et al.: Phys. Lett. 191 B (1987) 209; C. Buttar: Ph.D. thesis (1988)
4. CELLO Coll. H.J. Behrend et al.: Phys. Lett. 222 B (1989) 163; W. Wiedenmann: Ph.D. thesis, MPI-PAE/Exp. El. 195 (1988); S. Scholz: Ph.D. thesis, MPI-PAE/Exp. El. 222 (1990)
5. F. Cornet et al.: Phys. Lett. 174 B (1986) 224; F. Cornet, R. Rückl: Proc. Workshop on Physics at Future Accelerators, CERN 87-07, Vol. 2 (1987) 287
6. CELLO Coll. H.J. Behrend et al.: Z. Phys. C – Particles and Fields 47 (1990) 333
7. H. Kroha: Ph.D. thesis, MPI-PAE/Exp. El. 214 (1989)
8. UA1 Coll. C. Albajar et al.: Phys. Rev. Lett. 186 B (1987) 247
9. ARGUS Coll. H. Albrecht et al.: Phys. Lett. 192 B (1987) 245
10. CLEO Coll. M. Artuso et al.: Phys. Rev. Lett. 62 (1989) 2233
11. CELLO Coll. H.J. Behrend et al.: Phys. Lett. 183 B (1987) 400; G. d'Agostini, W. de Boer, G. Grindhammer: Phys. Lett. 229 B (1989) 160
12. W. de Boer: DESY 89-111 (1989)